



Cite this: *Chem. Commun.*, 2025, **61**, 15622

Received 15th August 2025,  
Accepted 2nd September 2025

DOI: 10.1039/d5cc04700e

rsc.li/chemcomm

Herein, we report a solid-state polycyclotrimerization of 1,4-diethynylbenzene using mechanochemical activation in a ball mill, yielding a highly porous and hydrophobic hyperbranched polymer (HBP) with a specific surface area of up to  $570\text{ m}^2\text{ g}^{-1}$ . The reaction, catalyzed by  $\text{Fe}(\text{hmds})_2$  and conducted under solvent-free conditions, was optimized by varying milling time and frequency. This method enables the efficient synthesis of insoluble, porous organic polymers with high yields (up to 95%) and offers an environmentally friendly alternative to traditional solution-based polymerizations.

Porous polymers have garnered significant research interest due to their ability to combine high surface area with tuneable chemical functionality. These materials are extremely versatile with applications in catalysis,<sup>1</sup> gas storage<sup>2</sup> and separation,<sup>3</sup> energy storage<sup>4</sup> and drug delivery.<sup>5</sup> Their fascination lies in their inherent flexibility, ductility and ability for precise functionalization. Typically, porous organic polymers (POPs) are synthesized by Friedel-Crafts alkylation,<sup>6</sup> transition metal-catalyzed reactions such as Sonogashira-Hagihara<sup>7</sup> and Suzuki-Miyaura cross-coupling<sup>8</sup> or Scholl oxidation.<sup>9</sup>

In addition, cyclotrimerization reactions are encountered across this and other areas of chemistry. These reactions offer notable atom economy and enable the formation of extended network structures. Examples include the condensation-driven trimerization of 1,4-phenylenediboronic acid resulting in the formation of COF-1,<sup>10</sup> aldol condensation leading to the formation of large covalent organic frameworks,<sup>11</sup> or the formation of covalent triazine frameworks (CTF), which primarily arise from the trimerization of nitriles.<sup>12</sup> The cyclotrimerization of alkynes commonly employs transition metal catalysts such as iron(II) bis(1,1,1,3,3,3-hexamethyldisilazide) ( $\text{Fe}(\text{hmds})_2$ ),<sup>13</sup> pyridinediimine iron complexes,<sup>14</sup> rhodium(III) chloride/amine,<sup>15</sup> ruthenium(II) complex<sup>16</sup> and many others.

## Solid-state polycyclotrimerization of diynes to porous organic polymers

Stefanie Hutsch,<sup>a</sup> Sven Grätz,<sup>id</sup><sup>a</sup> Jonas Lins,<sup>b</sup> Torsten Gutmann,<sup>id</sup><sup>b</sup> and Lars Borchardt,<sup>id,\*a</sup>

The polycyclotrimerization of diynes to form polymers involves similar catalyst such as cyclopentadienylcobaltdicarbonyl<sup>17</sup> or tantalum halides in combination with tetraphenyltin.<sup>18</sup> Traditional approaches typically employ toxic solvents like benzene<sup>19</sup> and are limited by monomer solubility and premature polymer precipitation, which hinder the formation of extended networks.

Mechanochemical methods offer a compelling alternative by initiating reactions through mechanical forces, eliminating the need for solvents and enabling reactions with poorly soluble monomers. Mechanochemistry has successfully been applied to reactions including Schiff base reaction,<sup>20</sup> Friedel-Crafts alkylation<sup>21,22</sup> or cyclotrimerization of nitriles.<sup>23</sup> Furthermore,

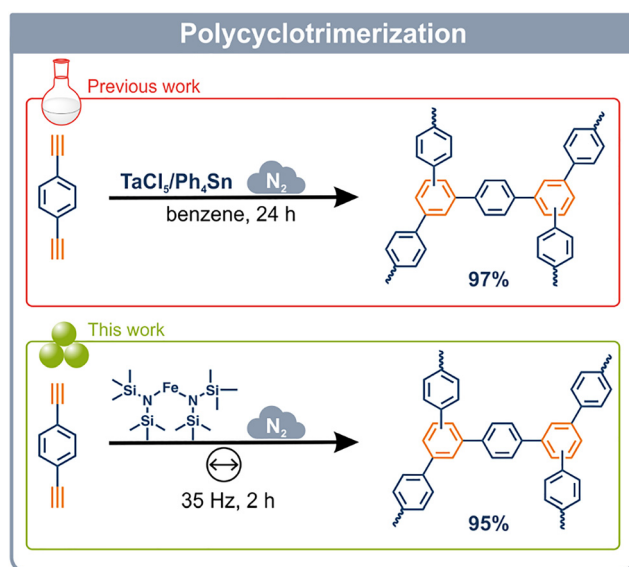


Fig. 1 Polycyclotrimerization of 1,4-diethynylbenzene. Up: solvent-based reaction utilizing  $\text{TaCl}_5/\text{Ph}_4\text{Sn}$  in benzene to obtain 97% yield.<sup>19</sup> Bottom: this work - solid state reaction utilizing  $\text{Fe}(\text{hmds})_2$  as catalyst. The reaction was conducted under nitrogen in an MM500 equipped with a 14 mL steel vessel containing a 10 mm steel ball at 30 Hz for 120 min.

<sup>a</sup> Inorganic Chemistry I Institute, Ruhr-Universität Bochum, Universitätsstrasse 150, 44801 Bochum, Germany. E-mail: lars.borchardt@ruhr-uni-bochum.de

<sup>b</sup> Institute for Inorganic and Physical Chemistry, Technical University Darmstadt, Peter-Grüning Strasse 8, 64287 Darmstadt, Germany



various polymerization reactions were adapted to mechanochemical approaches such as polycondensations<sup>24</sup> and ring-opening polymerizations,<sup>25</sup> thereby overcoming solubility issues compared to solution-based procedures. These methods have yielded numerous polymers as well as porous, functionalized materials, and represent a more environmentally friendly alternative to solvent-based syntheses.<sup>22</sup>

In this work, we present the first solid-state approach of the polycyclotrimerization of 1,4-diethynylbenzene (DEB) *via* ball mill (Fig. 1). The  $\text{Fe}(\text{hmds})_2$  catalyst was synthesized following a reported mechanochemical method,<sup>26</sup> involving the reaction of  $\text{FeCl}_2$  with two equivalents of lithium bis(trimethylsilyl)amide in the presence of a small amount of dioxane. The catalyst was purified by sublimation and subsequently used in a proof-of-principle reaction, conducted under nitrogen in an MM500 ball mill equipped with a 14 mL steel jar and a 10 mm steel ball. Milling at 30 Hz for 60 min yielded a light tan-colored, hydrophobic and porous hyperbranched polymer (HBP) with a yield of 61%. The polymer was characterized by FTIR spectroscopy, powder X-ray diffraction (PXRD),  $\text{N}_2$ , Ar and  $\text{H}_2\text{O}$  physisorption,  $^{13}\text{C}$  cross-polarization magnetic-angle-spinning (CP MAS) NMR and energy dispersive X-ray spectroscopy (EDX). The Fourier transform infrared (FTIR) spectrum exhibited a diminishing band at  $2105\text{ cm}^{-1}$  and a decreasing signal at  $3260\text{ cm}^{-1}$ , both associated with the  $-\text{C}\equiv\text{C}-\text{H}$  vibration (Fig. 2(I)). Additionally, the emergence of a new band at  $1600\text{ cm}^{-1}$ , assigned to aromatic  $\text{C}=\text{C}$  vibrations characteristic of trisubstituted benzene rings, is consistent with the successful cyclotrimerization of the alkyne units into aromatic structures. However, FTIR also revealed residual monomer in the products (see Fig. S1 and S2, SI), prompting refinement of the purification procedure. The best results were obtained when the crude products were washed with aqueous HCl and subsequently purified *via* Soxhlet extraction using ethyl acetate.

Subsequently, the porosity was characterized by nitrogen and argon physisorption measurements. According to the

IUPAC classification,  $\text{N}_2$  physisorption of HBP-60 min@30 Hz revealed a combination of type I and type II isotherms (Fig. S4, SI) and a  $\text{SSA}_{\text{BET}}$  of  $540\text{ m}^2\text{ g}^{-1}$  was quantified.<sup>27</sup> Similarly, the argon physisorption measurement shown in Fig. 2(II) demonstrated a  $\text{SSA}_{\text{BET}}$  of  $480\text{ m}^2\text{ g}^{-1}$ . The isotherm exhibited a steep uptake at low relative pressure highlighting the microporous character of the material. The narrow hysteresis loop suggests a rigid polymer network indicating a high degree of crosslinking. The pore size distribution was dominated by micropores of  $1.14\text{ nm}$  (Fig. S13, SI). In addition to  $\text{N}_2$  and Ar measurements,  $\text{H}_2\text{O}$  physisorption measurement was also performed. The resulting adsorption (Fig. S14, SI) corresponds to a type V isotherm characterized by a belayed uptake beginning at a relative pressure of 0.4. This behavior highlights the hydrophobic nature of the material (see also Fig. S24, SI). Moreover,  $^1\text{H}$ - $^{13}\text{C}$  CP MAS measurements were conducted, revealing three isotropic signals at 83 ppm, 129 ppm and 140 ppm with their spinning side bands marked by asterisks (Fig. 2(III)). The peak at 140 ppm corresponds to the substituted carbons labeled with b and c, while the signal at 129 ppm is assigned to the unsubstituted carbons a, d, and e. Additionally, the peak at 83 ppm represents the terminal carbons of the alkyne group (g and h).<sup>22,28</sup> Another small and broad signal is observed around 55 ppm which may be attributed to adsorbed ethyl acetate. Afterwards, the morphology of the polymer was analyzed by PXRD (Fig. S3, SI) illustrating the amorphous character of HBP-60 min@30 Hz. Finally, the EDX spectrum and mapping (Fig. S16-S23 and Table S2, SI) confirmed pure carbon material without detectable impurities from the catalyst or bulk material.

To enhance mixing, lithium chloride (a catalyst synthesis byproduct) was added as bulk material. Parallel reactions using crude and purified  $\text{Fe}(\text{hmds})_2$  yielded hydrophobic powders with surface areas of  $490$  and  $425\text{ m}^2\text{ g}^{-1}$ , respectively. Crude catalyst was used for subsequent experiments due to similar polymer properties.

Porous material may be sensitive to mechanical stress, as the porous network could be destroyed by shear forces or

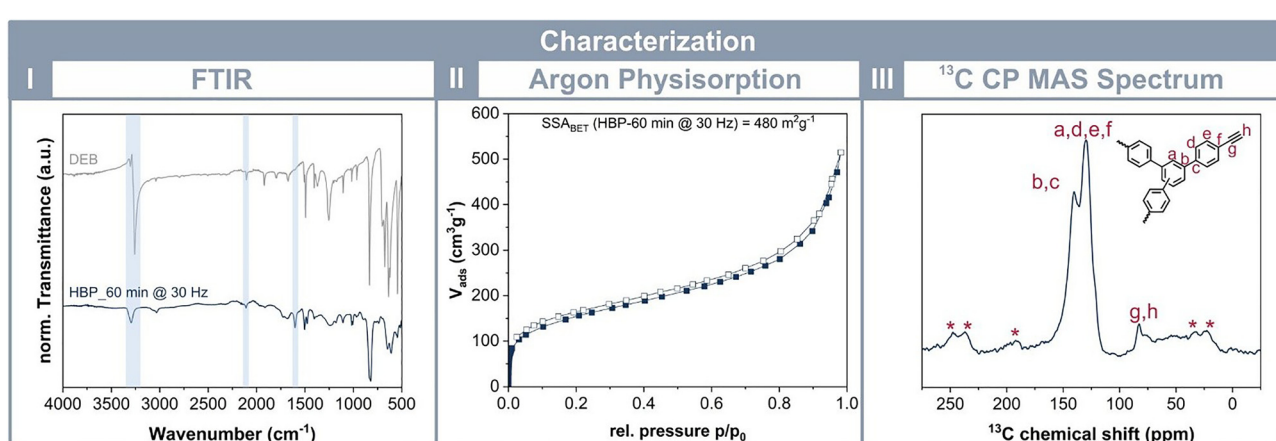


Fig. 2 Characterization of the obtained HBP-60 min@30 Hz. (I) Fourier transformed infrared spectrum of the monomer 1,4-diethynylbenzene (light grey) and HBP-60 min@30 Hz (dark blue). (II) Ar physisorption mixed type I and II isotherm at 87 K with a  $\text{SSA}_{\text{BET}}$  of  $480\text{ m}^2\text{ g}^{-1}$ . (III)  $^{13}\text{C}$  cross-polarization magnetic-angle-spinning (CP MAS) spectrum of HBP-60 min@30 Hz measured at 8 kHz spinning. The isotropic signals at 83 ppm, 129 ppm and 140 ppm are labeled with letters (a–h), and signals marked with asterisks are spinning side bands according to SI Fig. S15.

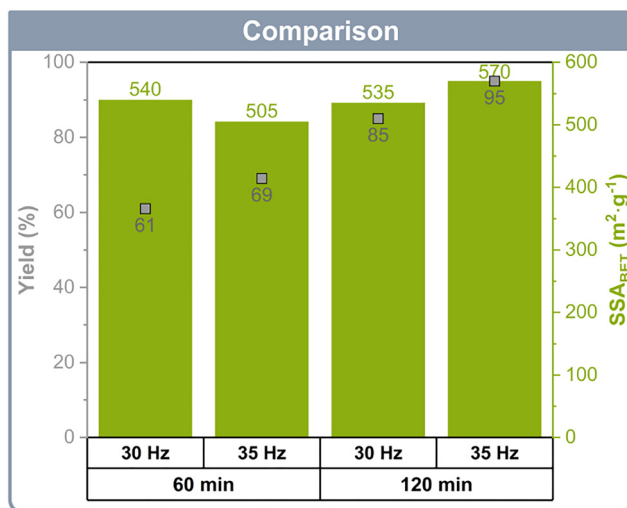


Fig. 3 Comparison of parameter influence: the yield is shown as black framed grey dots, and the green columns show the SSA<sub>BET</sub> of the obtained HBP. The yields of the HBPs obtained with a reaction time of 120 min are higher, while the SSA<sub>BET</sub> for the HBPs synthesized with a frequency of 35 Hz are slightly increased.

mechanical impact.<sup>29</sup> To examine the impact of mechanical stress on HBP, we varied reaction times and frequencies.

Extending milling to 120 min at 30 Hz increased yield to 85% but slightly reduced surface area to 505 m<sup>2</sup> g<sup>-1</sup>, possibly due to partial framework degradation. FTIR and PXRD, however, displayed similar characteristics to those of HBP-60 min@30 Hz (Fig. S1–S3; SI). At 35 Hz, the 60 min reaction (HBP-60 min@35 Hz) resulted in a slightly higher yield of 69% compared to HBP-60 min@30 Hz (Fig. 3). In contrast, the 120 min reaction at 35 Hz yielded 95% of the polymer, comparable to HBP-120 min@30 Hz. These results indicate that a 120-minute reaction time is required for complete conversion. An improvement in the SSA<sub>BET</sub> was observed when comparing the porosity of the HBPs synthesized at 30 Hz with those obtained at 35 Hz. The two specific surface areas of 565 m<sup>2</sup> g<sup>-1</sup> (HBP-60 min@35 Hz) and 570 m<sup>2</sup> g<sup>-1</sup> (HBP-120 min@35 Hz) are nearly identical (Fig. 3) with no indication of degradation in the porous network due to the increased frequency. In comparison to solution-based polymers, the SSA<sub>BET</sub> of the mechanochemical HBP is lower. For instance, polymers obtained using Co<sub>2</sub>(CO)<sub>8</sub> exhibit an SSA<sub>BET</sub> of 1031 m<sup>2</sup> g<sup>-1</sup>,<sup>30</sup> while those synthesized with TaCl<sub>5</sub>/Ph<sub>4</sub>Sn reach 1299 m<sup>2</sup> g<sup>-1</sup>.<sup>19</sup> However, these methods require either harsh conditions, such as reaction temperatures of 125 °C and highly toxic catalysts,<sup>30</sup> or long reaction times of up to 24 hours,<sup>19</sup> highlighting the mechanochemical route as a mild and fast alternative to solution-based procedures.

Some further experiments were conducted with variations in parameter, including liquid-assisted grinding (LAG). This method is commonly employed in mechanochemistry to accelerate reactions by adding a small amount of liquid. In this case, 140 µL of benzotrifluoride was added to the reaction mixture, corresponding to an  $\eta$  - value of 0.2 µL mg<sup>-1</sup>. The reaction was

then conducted for 120 min at 35 Hz. The SSA<sub>BET</sub> was 575 m<sup>2</sup> g<sup>-1</sup>, which is comparable to that of HBP-120 min@35 Hz synthesized without LAG. However, the yield decreased significantly from 95% to 59% upon application of LAG indicating a negative influence on the reaction efficiency. A possible explanation could be a side reaction with benzotrifluoride, leading to partial consumption of the catalyst. In the next experiment, the bulk material was replaced with sodium chloride, a more ecological alternative to lithium chloride. The polymer was obtained with 98% yield and the SSA<sub>BET</sub> reached 590 m<sup>2</sup> g<sup>-1</sup> demonstrating comparable results to those achieved using LiCl as bulk material. Finally, the monomer amount was increased from 1 mmol to 8 mmol to investigate the scalability of the reaction. Accordingly, the reaction vessel volume was adjusted to 20 mL. This modification proved beneficial, as the HBP, obtained in 84% yield, exhibited an increased SSA<sub>BET</sub> of 640 m<sup>2</sup> g<sup>-1</sup>.

In conclusion, this work demonstrates the first mechanochemical route to hyperbranched porous polymers *via* solid-state alkyne polycyclotrimerization. The method utilizes a ball mill and Fe(hmds)<sub>2</sub> in a short reaction time of 120 min to obtain highly hydrophobic and porous polymers with a SSA<sub>BET</sub> of up to 570 m<sup>2</sup> g<sup>-1</sup> and quantitative yields. This approach circumvents toxic solvents making it a scalable and sustainable alternative for various insoluble monomers.

We gratefully acknowledge the German Research Foundation, Deutsche Forschungsgesellschaft (DFG), for the funding of the project under DFG BO 4538/8-1 and DFG GU-1650/3-2.

## Conflicts of interest

There are no conflicts to declare.

## Data availability

The data supporting this article have been included as part of the SI. See DOI: <https://doi.org/10.1039/d5cc04700e>.

## References

- 1 S.-Y. Ding, J. Gao, Q. Wang, Y. Zhang, W.-G. Song, C.-Y. Su and W. Wang, *J. Am. Chem. Soc.*, 2011, **133**, 19816–19822.
- 2 H. Furukawa and O. M. Yaghi, *J. Am. Chem. Soc.*, 2009, **131**, 8875–8883.
- 3 Y. Zhao, X. Liu and Y. Han, *RSC Adv.*, 2015, **5**, 30310–30330.
- 4 M. Chafiq, A. Chaouiki and Y. G. Ko, *Energy Storage Mater.*, 2023, **63**, 103014.
- 5 Q. Fang, J. Wang, S. Gu, R. B. Kaspar, Z. Zhuang, J. Zheng, H. Guo, S. Qiu and Y. Yan, *J. Am. Chem. Soc.*, 2015, **137**, 8352–8355.
- 6 Z. Jia, J. Pan and D. Yuan, *ChemistryOpen*, 2017, **6**, 554–561.
- 7 (a) J.-X. Jiang, F. Su, A. Trewin, C. D. Wood, H. Niu, J. T. A. Jones, Y. Z. Khimyak and A. I. Cooper, *J. Am. Chem. Soc.*, 2008, **130**, 7710–7720; (b) K. Zhang, B. Tieke, F. Vilela and P. J. Skabar, *Macromol. Rapid Commun.*, 2011, **32**, 825–830.
- 8 Q. Chen and B.-H. Han, *Macromol. Rapid Commun.*, 2018, **39**, e1800040.
- 9 (a) M. Grzybowski, B. Sadowski, H. Butenschön and D. T. Gryko, *Angew. Chem., Int. Ed.*, 2020, **59**, 2998–3027; (b) B. Li, Z. Guan, X. Yang, W. D. Wang, W. Wang, I. Hussain, K. Song, B. Tan and T. Li, *J. Mater. Chem. A*, 2014, **2**, 11930.
- 10 A. P. Côté, A. I. Benin, N. W. Ockwig, M. O'Keeffe, A. Matzger and O. M. Yaghi, *Science*, 2005, **310**, 1166–1170.



- 11 (a) M. Rose, N. Klein, I. Senkovska, C. Schrage, P. Wollmann, W. Böhlmann, B. Böhringer, S. Fichtner and S. Kaskel, *J. Mater. Chem.*, 2011, **21**, 711–716; (b) F. M. Wisser, K. Eckhardt, D. Wisser, W. Böhlmann, J. Grothe, E. Brunner and S. Kaskel, *Macromolecules*, 2014, **47**, 4210–4216.
- 12 (a) P. Kuhn, M. Antonietti and A. Thomas, *Angew. Chem., Int. Ed.*, 2008, **47**, 3450–3453; (b) B. J. Smith, A. C. Overholts, N. Hwang and W. R. Dichtel, *Chem. Commun.*, 2016, **52**, 3690–3693.
- 13 D. Brenna, M. Villa, T. N. Gieshoff, F. Fischer, M. Hapke and A. Jacobi von Wangelin, *Angew. Chem., Int. Ed.*, 2017, **129**, 8571–8574.
- 14 J. S. Doll, R. Eichelmann, L. E. Hertwig, T. Bender, V. J. Kohler, E. Bill, H. Wadeppohl and D.-A. Roșca, *ACS Catal.*, 2021, **11**, 5593–5600.
- 15 K. Yoshida, I. Morimoto, K. Mitsudo and H. Tanaka, *Chem. Lett.*, 2007, **36**, 998–999.
- 16 Y. Yamamoto, T. Arakawa, R. Ogawa and K. Itoh, *J. Am. Chem. Soc.*, 2003, **125**, 12143–12160.
- 17 K. Xu, H. Peng, Q. Sun, Y. Dong, F. Salhi, J. Luo, J. Chen, Y. Huang, D. Zhang, Z. Xu and B. Z. Tang, *Macromolecules*, 2002, **35**, 5821–5834.
- 18 M. Häufeler, J. Liu, J. W. Y. Lam, A. Qin, R. Zheng and B. Z. Tang, *J. Polym. Sci. A*, 2007, **45**, 4249–4263.
- 19 A. Zukal, E. Slováková, H. Balcar and J. Sedláček, *Macromol. Chem. Phys.*, 2013, **214**, 2016–2026.
- 20 S. Chandra, S. Kandambeth, B. P. Biswal, B. Lukose, S. M. Kunjir, M. Chaudhary, R. Babarao, T. Heine and R. Banerjee, *J. Am. Chem. Soc.*, 2013, **135**, 17853–17861.
- 21 S. Grätz, S. Zink, H. Kraffczyk, M. Rose and L. Borchardt, *Beilstein J. Org. Chem.*, 2019, **15**, 1154–1161.
- 22 A. Krusenbaum, J. Geisler, F. J. L. Kraus, S. Grätz, M. V. Höfler, T. Gutmann and L. Borchardt, *J. Polym. Sci.*, 2022, **60**, 62–71.
- 23 S. Hutsch, A. Leonard, S. Grätz, M. V. Höfler, T. Gutmann and L. Borchardt, *Angew. Chem., Int. Ed.*, 2024, **63**, e202403649.
- 24 S. Grätz and L. Borchardt, *RSC Adv.*, 2016, **6**, 64799–64802.
- 25 N. Ohn, J. Shin, S. S. Kim and J. G. Kim, *ChemSusChem*, 2017, **10**, 3529–3533.
- 26 J. A. Cabeza, J. F. Reynes, F. García, P. García-Álvarez and R. García-Soriano, *Chem. Sci.*, 2023, **14**, 12477–12483.
- 27 M. Thommes, K. Kaneko, A. V. Neimark, J. P. Olivier, F. Rodriguez-Reinosa, J. Rouquerol and K. S. Sing, *Pure Appl. Chem.*, 2015, **87**, 1051–1069.
- 28 A. Krusenbaum, F. J. L. Kraus, S. Hutsch, S. Grätz, M. V. Höfler, T. Gutmann and L. Borchardt, *Adv. Sustainable Syst.*, 2023, 2200477.
- 29 (a) A. Krusenbaum, S. Grätz, S. Bimmermann, S. Hutsch and L. Borchardt, *RSC Adv.*, 2020, **10**, 25509–25516; (b) A. Krusenbaum, S. Grätz, G. T. Tigineh, L. Borchardt and J. G. Kim, *Chem. Soc. Rev.*, 2022, **51**, 2873–2905.
- 30 S. Yuan, B. Dorney, D. White, S. Kirklin, P. Zapol, L. Yu and D.-J. Liu, *Chem. Commun.*, 2010, **46**, 4547–4549.

